Progress in Satellite Attitude Determination and Control
人工衛星の姿勢決定と制御における進歩

Jozef C. VAN DER HA
Department of Aeronautics and Astronautics, Kyushu University

Key Words : Satellites, Operations, Attitude Determination, Attitude Control

要旨：本解説は，宇宙機の姿勢決定と制御の分野から，いくつかのトピックを取り上げ紹介する．著者は，欧州宇宙機関（ESA）や米国航空宇宙局（NASA）の人工衛星を，過去30年にわたり数多く設計・運用してきた．本稿のトピックは，その経験の中から選んだ．スピン安定衛星と3軸安定衛星は，姿勢決定と制御に大変異なる概念と方法を用いているが，本稿はその両方をカバーする．

スピン安定は魅力的な方式である．なぜなら，ジャイロ剛性が外乱トルクに対するロバスト性を提供するからである．この点は，高推力の固体ロケットモータや2液式エンジンによる軌道投入マヌーバの際に，特に重要となる．スピン軸方向の正確な決定と制御が，噴射後目標とする軌道に到達するのに必要な，精密な軌道速度増分を得るのに欠かせないからである．本稿では，最もよく使われているアプローチである太陽センサと地球センサを用いたスピン軸姿勢決定について，主要な側面を紹介する．また，スピン軸方向を制御する最も実用的な手法にも言及する．航程線マヌーバと呼ぶこのアプローチは，太陽センサ信号と同期したパルスモードで，スラスタを噴射することで実現される．

本稿の後半では，3軸姿勢安定に焦点を当てる．TRIAD法やQUEST法は，よく使われている姿勢決定アルゴリズムであり，大変有効である．しかしながら，これらを使うことができるのは，空間に固定された基準姿勢に対して計測する場合のみである．一方，カルマンフィルタとして知られる推定方法は，より柔軟で，急速に変化する姿勢にも対応できる．厳しい姿勢要求が課されている3軸安定ミッションには，センサという点では，恒星センサが必要である．それほど厳しくない精度要求のミッションの場合は，太陽センサと磁気センサが，低コストの選択肢となる．本稿では，最後に，地球磁場を用いた3軸姿勢決定と制御の方法を紹介する．これらのアプローチは，数degレベルの比較的中程度の指向決定・制御性能しか提供しないが，低コストで設計が簡単であるという理由で魅力的である．

1. INTRODUCTION

This review paper presents a personal account of some of the progress made in the field of attitude determination and control of actual spacecraft during the last 30 years. The paper covers spin-stabilized as well as three-axis-stabilized spacecraft. The topics are mainly taken from the author's experiences in the design and operations of a number of ESA and NASA satellites.

The reference book[1] *Spacecraft Attitude Determination and Control*, edited by J. Wertz, provides a comprehensive overview of the state of the art of spacecraft attitude determination and control during the late 1970's. Whereas the book's contents are still largely valid and relevant even today, the capabilities and complexities of satellites have evolved enormously over the last 30 years. In particular, on-board computing power, in a very primitive state when Wertz's book appeared, has increased by many orders of magnitude. Sophisticated sensors are now available at much lower cost than the relatively primitive devices of the 1970's. For instance, autonomous star sensors that can establish a satellite's attitude without any prior knowledge within less than 10 seconds can now be procured at a very moderate cost. Furthermore, the emergence of small low-cost satellites during the last decade has lead to many novel design and operating concepts. In particular, efficient three-axis attitude determination and control in Low Earth Orbit (LEO) is possible by utilizing magnetometers as sensors and magnetic torquers as actuators.

The first part of this paper addresses the attitude determination and control of spin-stabilized spacecraft. Many satellites employ spin-stabilization during at least part of their lifetime. For instance, most geostationary spacecraft use a spinning mode during their Geostationary Transfer Orbit (GTO) phases before they are injected into their operational geostationary orbits.

Spin-stabilization is an attractive technique because the gyroscopic stability provides inherent robustness against external disturbance torques. Therefore, in contrast to three-axis stabilized satellites, spin-stabilized spacecraft have no need for additional safe attitudes modes. Spin-stabilization is particularly effective for providing pointing stability during orbit injection maneuvers using high-thrust solid rocket motors or bipropellant engines. Attitude pointing requirements during these maneuvers vary from 0.5 to 1 degree. A pointing error in the spin-axis attitude during the injection maneuver leads to a

Received on November 28th, 2007

trajectory error which must be corrected afterwards by using on-board propellant. This reduces the propellant available during the mission operations phase. Therefore, the accurate determination of the spin-axis attitude and the correction of the attitude error before performing orbit injection maneuvers has benefits for the satellite's lifetime[2].

The paper provides the essential aspects of spin-axis attitude determination using Sun and Earth sensors which is the approach used by most spacecraft. Furthermore, an overview of spin-axis attitude control using rhumb-line maneuvers will be presented.

The second part of the paper examines three-axis attitude determination and control. Well-established classical three-axis attitude determination algorithms like TRIAD[3] and QUEST[3] are relatively easy to implement and have been used successfully in many satellite missions. However, both of these methods start from the inherent assumption that the measurements originate from a fixed attitude orientation in space.

In practice, the attitude orientation usually varies over time. For these applications, the most widely used attitude estimation algorithm is the well known Kalman Filter (KF). Reference 4) gives a general formulation of the Extended Kalman Filter (EKF) method for attitude-determination applications. A comprehensive up-to-date review[5] of nonlinear estimation methods for attitude-determination purposes was published recently.

For missions with demanding real-time attitude determination requirements at a level of below about 20 arcsec, a star sensor would be needed. Nowadays, off-the-shelf star sensors deliver the instantaneous optimal attitude quaternion (by using QUEST or a similar algorithm) instead of the individual star position measurements. In this manner, the star sensor delivers 'attitude measurements' that may subsequently be processed along with other measurements from different sensors using a KF[6]. This has been a common approach for many interplanetary missions during the past decade.

For three-axis stabilized missions with less stringent accuracy requirements, typical cost-effective sensors would be three-axis Sun-sensors and magnetometers. In the final section of the paper, we summarize three-axis attitude determination and control methods that make use of the Earth's magnetic field. Although the achievable pointing accuracies are relatively modest (typically, a few degrees), these approaches are attractive because of their simplicity and the lack of on-board propellant. Magnetic attitude determination and control is mainly used by nano- and micro-satellites in Low Earth Orbit (LEO).

2. SPIN-AXIS ATTITUDE DETERMINATION

2.1. Attitude Measurement Equations

The determination of the spin-axis orientation normally makes use of Sun- and Earth-sensor measurements. A typical (V-slit) Sun sensor for spinning satellites has a vertical and a skew slit. The Sun's crossing times over these two slits are measured by silicon photo-detectors. Successive vertical slit crossings provide the spin-rate measurement. The Sun-aspect angle θ is obtained from the time difference between successive vertical and skew slit crossings by using spherical geometry (Wertz[1], § 7.1.1). The Sun-aspect angle represents the most common measurement for the attitude determination of spinning satellites. It is defined as the angle between the spin axis and the Sun direction (Fig. 1):

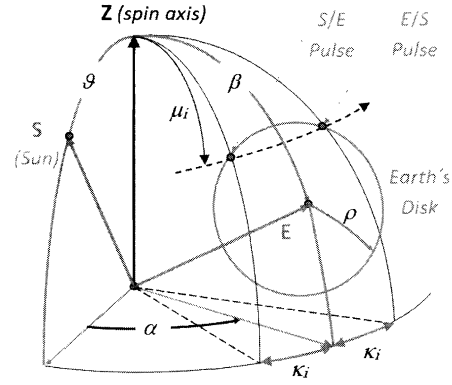

Fig. 1. Sun and Earth-sensor measurements θ, β, α.

$$\theta = \arccos\{\boldsymbol{Z}\cdot\boldsymbol{S}\} \quad (1)$$

The typical Earth sensor for spinning satellites has two (static) pencil-beams which are oriented at the angles μ_i ($i=1, 2$) relative to the spin axis (Fig. 1). The sensor outputs are produced by bolometer detectors measuring the Earth's radiation in the CO_2 band of the infra-red part of the spectrum. This band is selected because of its limited variability in radiance under seasonal and weather influences (Wertz[1], §4.2).

The instants of time at which the Earth-sensor detectors cross the Space/Earth (S/E) and Earth/Space (E/S) boundaries are calculated by on-board signal processing. These crossing pulses represent the fundamental Earth sensor measurements and are downlinked in the telemetry data. With our knowledge of the spin-rate we can express these pencil-beam crossing pulses in the chord-angles κ_i ($i=1, 2$), which are the measurement angles used by the attitude determination software. Spherical geometry in the triangle formed by the vectors $\boldsymbol{Z}$, $\boldsymbol{E}$, and the S/E or E/S directions in Fig. 1 gives the relationship (Wertz[1], equation 11.7):

$$\cos\mu_i\cos\beta+\sin\mu_i\sin\beta\cos\kappa_i=\cos\rho \quad (i=1,2) \quad (2)$$

The angle ρ represents the apparent Earth radius seen from the satellite. The Earth-aspect angle (or nadir angle) β is the angle between the spin-axis $\boldsymbol{Z}$ and the spacecraft-to-Earth unit-vector (or simply the Earth-vector) $\boldsymbol{E}$ shown in Fig. 1:

$$\beta(\nu) = \arccos\{\boldsymbol{Z}\cdot\boldsymbol{E}(\nu)\} \quad (3)$$

The Earth-vector $\boldsymbol{E}$ points opposite to the instantaneous

orbital radius vector and rotates along with the satellite's orbital phase angle ν. Its evolution is known from the orbit determination.

Equations (2) offer an implicit functional relationship for the calculation of the Earth-aspect angle β from the two fundamental half-chord angle measurements κ_i $(i=1, 2)$. This may be achieved, for instance, by means of a differential correction algorithm using a priori attitude knowledge[7].

The geometry of the Sun and Earth measurements shown in Fig. 1 produces another independent measurement, namely the Sun-Earth dihedral angle α. This rotation angle represents the delay between the Sun sensor's vertical slit measuring the Sun's crossing and the Earth sensor observing the Earth-center crossing. The latter event follows from the average of the S/E and E/S crossings (which may also be averaged for the two pencil-beams). Spherical geometry in the triangle formed by the $\boldsymbol{S}$, $\boldsymbol{E}$, and $\boldsymbol{Z}$ unit-vectors produces an intricate measurement equation between α and $\boldsymbol{Z}$ which involves also the measurement angles θ and β:

$$\alpha(\nu)=\arcsin\{\boldsymbol{Z}\cdot(\boldsymbol{S}\times\boldsymbol{E})/(\sin\theta\sin\beta)\} \qquad (4)$$

Finally, we summarize the three measurement equations (1), (3) and (4) in the form of a linear system of equations:

$$\boldsymbol{y}=H\boldsymbol{Z} \qquad (5a)$$

with:

$$\boldsymbol{y}=\begin{pmatrix}\cos\theta\\ \cos\beta\\ \sin\theta\sin\beta\sin\alpha\end{pmatrix}; \qquad (5b)$$

$$H=\begin{pmatrix}S_1 & S_2 & S_3\\ E_1 & E_2 & E_3\\ (\boldsymbol{S}\times\boldsymbol{E})_1 & (\boldsymbol{S}\times\boldsymbol{E})_2 & (\boldsymbol{S}\times\boldsymbol{E})_3\end{pmatrix} \qquad (5c)$$

The indices 1, 2, and 3 denote the components of the respective vectors in the adopted inertial reference frame.

2.2. Attitude Determination Methods

We assume that the reference vectors $\boldsymbol{S}$ and $\boldsymbol{E}$ are not aligned. In that case, the system of equations (5a) is non-singular and the matrix H can be inverted. The inertial attitude vector follows now immediately as $\boldsymbol{Z}=H^{-1}\boldsymbol{y}$ in terms of the θ, β, α angles through equation (5b). This represents a *single-frame* attitude solution because the measurements are collected at a single instant of time.

In practice, a batch of n measurements θ_j, β_j, α_j $(j=1, \cdots, n)$ will be collected over n satellite spin periods. This gives an over-determined system of equations with n times the three equations (5a) for the three unknown components of the attitude vector $\boldsymbol{Z}$. After the addition of random errors to the measurement equations (5a), it will be possible to determine the optimal attitude estimate, for instance with the help of a weighted-least-square method[7,8]. Because the attitude vector $\boldsymbol{Z}$ is a unit-vector, normalization must still be performed afterwards.

Reference 8) offers a few efficient single-frame and batch least-square attitude solutions on the basis of the system of equations in (5a). Also meaningful covariance matrices of the attitude solutions are presented. Reference 9) provides a more recent survey of attitude determination methods for spinning satellites.

For illustration, we refer to the attitude determination approach that was implemented for the CONTOUR comet probe[7]. The Earth-sensor design was customized for the CONTOUR-specific Earth-phasing orbits with relatively high apogees of 116000 km. The Earth-sensor delivers its optimal performance in the altitude range from 50000 to 60000 km, which corresponds to the Earth-sensor coverage interval for CONTOUR's nominal injection attitude (and its pencil-beam settings of 60 and 65 degrees).

Figure 2 shows the predicted half-chord measurement angles κ_i $(i=1, 2)$ generated by the Earth sensor in accordance with equation (2). The independent variable is the Earth-aspect angle β which decreases as a function of time during the post-apogee Earth-sensor coverage interval[7]. Fig. 2 also shows the apparent Earth-radius angle ρ with its increasing trend over this part of the orbit.

The difference in the pencil-beam orientation angles causes the shift in the respective Earth-sensor coverage intervals by about 5 degrees over the orbit (see Fig. 2). Scans over the mid-latitude region of the Earth provide the most favorable conditions. The small chords have a relatively high systematic error due to the near-tangential Earth crossings. On the other hand, singularities occur in the calculation of β from κ_i $(i=1, 2)$ near the maxima of the chords because of the low geometrical sensitivity (see Fig. 2).

Two different attitude determination methods were employed during CONTOUR's Earth-phasing orbits in summer 2002:

a) The *Equal-Chord Method*[10] provides the Earth-aspect angle at the single point in the coverage interval where the two chords generated by the two pencil-beams are equal (at $\beta\approx62.6°$, Fig. 2). The two equations (2) produce a straightforward solution for the Earth-Aspect

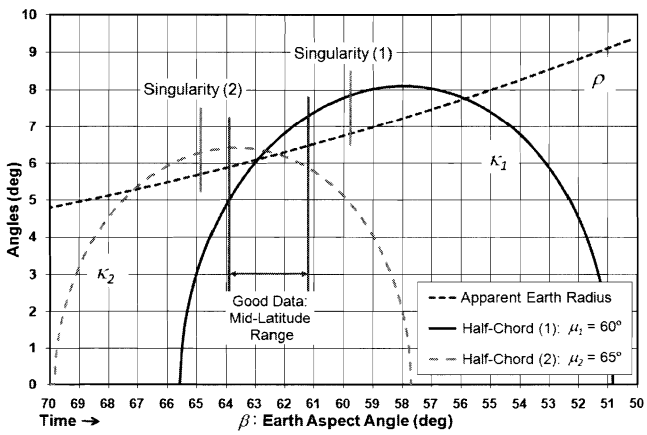

Fig. 2. Evolution of half-chord angles and apparent Earth radius.

angle β_e at the equal-chord time t_e:

$$\beta_e = \arctan\{\tan\mu/\cos\kappa_e\} \text{ with: } \mu = (\mu_1+\mu_2)/2 \quad (6)$$

By including the measurements of the angles θ_e and α_e at the time t_e, we have a system of equations as in Eqs. (5). Therefore, we get the attitude estimate by applying the single-frame geometrical method presented above, at the time t_e. CONTOUR's in-orbit experience has demonstrated and validated the effectiveness of the Equal-Chord Method[10]. Its results are insensitive to uniform biases in the Earth's infra-red horizon and the accuracy of its results is comparable to that of more elaborate methods[7,10].

b) The *Fine Attitude Determination* method uses a half-hour long batch of Sun- and Earth-sensor measurement data collected in the mid-latitude region (Fig. 2). A precise attitude estimate is established by means of a weighted-least-square algorithm[7].

A very different attitude determination method was developed for CONTOUR's deep-space trajectory when the Earth sensor cannot be used, namely the *Two-Sun-Cones Method*[11,12]. This method establishes complete attitude knowledge using only Sun-sensor measurements by using two different Sun-aspect angles at two instants of time a few hours or days apart. These Sun angles identify two nearly identical cones similarly to the Sun and Earth cones used in equations (5). The spin-axis attitude points along one of the intersections of these cones. The method offers good accuracy (well below 1 degree) after a one-day interval[11].

2.3. Measurement Errors

Measurement errors may be categorized in terms of random errors and systematic errors (also known as *biases*). Random errors are generated by stochastic fluctuations in the realizations of a measurement whereas the (systematic) biases originate from imperfections in the state and measurement models. The influence of random errors on the attitude estimation accuracy can essentially be eliminated by simply considering a sufficiently large batch of measurement data.

Biases, on the other hand, are much more serious, since their adverse effects cannot be eliminated easily. In fact, biases often cannot even be observed unambiguously. Sources for bias errors are manifold: for instance, misalignments, electronic triggering delays, processing effects, sensor calibration limitations, spin-axis dynamical imbalance (due to uncertainties in the inertias), deviations in the Earth's infra-red profile, orbit determination and Sun ephemeris errors. In order to be able to assess the accuracy of the attitude determination, it is important that we understand the propagation of the dominant biases into the attitude estimate. This may be accomplished by means of covariance analysis[2,13].

The main error contributions are often due to the Earth's infra-red horizon biases which may be up to 0.3 deg along the north-south scanning direction. Spin-axis dynamic imbalance errors (including imbalances in the propellant tanks) may be about 0.1 deg and other bias errors are typically somewhat smaller.

3. SPIN-AXIS ATTITUDE CONTROL

The launcher usually releases the spacecraft in an attitude which is different from the one needed for the subsequent orbit injection (by on-board solid rocket motor or thrusters). Therefore, attitude reorientation maneuvers must be performed. Furthermore, orbit maneuvers may be needed for correcting launcher injection errors. This would require additional attitude maneuvers in order to point the thrust vector in the desired $\Delta \boldsymbol{v}$ direction. For instance, during CONTOUR's six weeks of Earth-phasing orbits, seven orbit and twelve attitude maneuvers were performed in total[7].

The attitude control of a spin-stabilized spacecraft is usually accomplished by a forced precession of the spin axis induced by a series of thruster pulses which are synchronized with the spin phase angle[14]. The inertial direction of the spin-axis motion is controlled by the delay time t_c (with spin phase angle φ_c) in the start of the thruster firings relative to the instant when the Sun crosses the Sun-sensor's vertical slit (which happens when the spacecraft x-axis crosses the inertial x_S axis in Fig. 3). The delay is prepared on-ground and uplinked along with the number and durations of thrust pulses. If the delay angle remains constant during the maneuver, the spin-axis motion follows a rhumb-line (or loxodrome) path on the unit-sphere (Wertz[1], pp. 651-654). The thruster locations and thrust directions define the angle τ[14].

Figure 4 illustrates the path of a rhumb-line maneuver on the celestial sphere. The maneuver path makes a constant rhumb (or heading) angle χ from the 'Sun cone', which is the local latitude parallel on the sphere with the Sun placed at its north pole.

Reference 14) gives a detailed error propagation model based on the mathematical equations of an arbitrary rhumb-line maneuver:

$$\theta_f(\lambda_f,\chi,\theta_i) = \theta_i - \lambda_f \sin\chi$$
$$\xi_f(\lambda_f,\chi,\theta_i,\xi_i) = \xi_i - \{y(\theta_f) - y(\theta_i)\}/\tan\chi \quad (7)$$

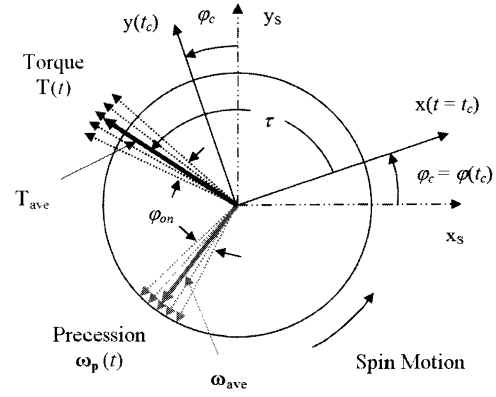

Fig. 3. Geometry of torque and precession vectors.

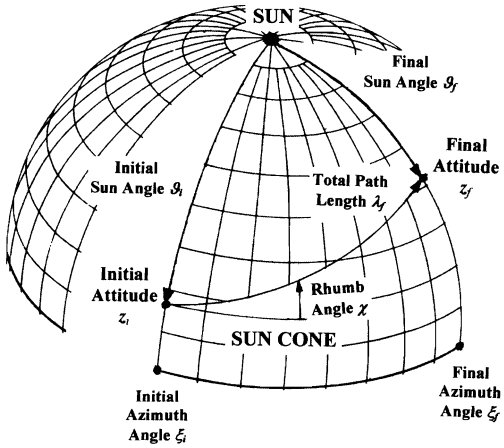

Fig. 4. Geometry of rhumb-line maneuver.

The function $y(\theta)$ denotes $ln[\tan \theta/2]$ and the other symbols are defined in Fig. 4. The maneuver path-length λ_f is proportional to the number and the magnitude of the applied thrust pulses[14]. Therefore, errors in the intended thrust level lead to errors in the resulting path-length. Similarly, the maneuver's rhumb angle χ consists of the sum of the delay angle and the centroid time (i.e., mid-time) of the thrust pulses[14]. Errors in these two parameters lead to proportional errors in the effective rhumb angle.

The satellite system design often imposes constraints on the permissible attitude orientation due to system-level requirements (for example, power). This means that the potential excursions of the attitude pointing direction during the maneuver must be maintained within some narrow bounds relative to the intended nominal path. Therefore, careful calibrations of the effective thrust level and centroid time (as well as the spin rate) must be carried out before the execution of long attitude maneuvers.

During CONTOUR's initial operations, an elaborate maneuver calibration technique was performed before performing a 180° long maneuver[7]. The calibrations took advantage of the accurate Sun-aspect angle measurements produced by the Sun-sensor with random noise of 0.003 deg (rms). The objective of the first calibration maneuver was the calibration of the thrust level. The maneuver path headed normal to the local Sun cone and the Sun sensor measured its path-length accurately. The next calibration maneuver established the centroid time of the thrust pulses. It used a nominal path along the local Sun cone direction and the Sun sensor measured the deviation from this path accurately which gives the actual rhumb angle. As a result, CONTOUR's two 180° maneuvers achieved their targets within 3 degrees[7].

4. THREE-AXIS ATTITUDE DETERMINATION

The attitude of a three-axis stabilized spacecraft in an inertial reference frame can be described completely and

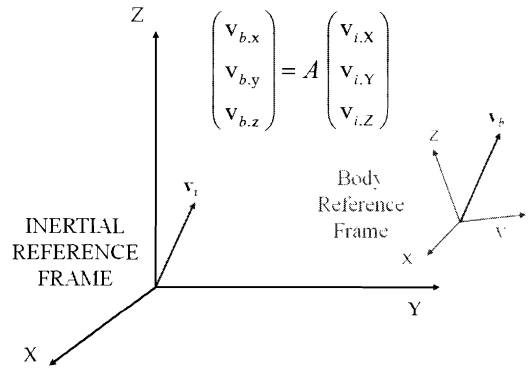

Fig. 5. Illustration of measurement and reference vectors.

uniquely by three independent parameters[15]. Attitude determination is often achieved with the help of external reference directions. These directions are observed by sensors that are rigidly attached to the spacecraft. For instance, Sun, Earth, or star sensors measure the directions to the Sun, Earth, or a set of stars, respectively, in the spacecraft reference frame. Also the direction of the geomagnetic field vector can be measured by using an on-board magnetometer. A reference direction represents a unit-vector defined by two parameters (for example, right ascension and declination). Thus, the three unknown attitude parameters can be calculated from at least two independent reference directions. These provide already more information than would strictly be needed.

4.1. Algebraic or TRIAD Method

The oldest and simplest three-axis attitude determination method, developed in 1964 by Black[16], is the *algebraic method* (Wertz[1], § 12.2.2). This method is also known as the TRIAD algorithm[3]. It uses two unit-vector measurements $\boldsymbol{v}_b^{(1)}$ and $\boldsymbol{v}_b^{(2)}$ generated by on-board sensors along with the associated known reference vectors $\boldsymbol{v}_i^{(1)}$ and $\boldsymbol{v}_i^{(2)}$. The reference vectors are usually defined in a geocentric inertial reference frame, but any other well-defined frame may be used as well. The Sun, Earth, star, or magnetic-field measurements are produced by the relevant sensor, whereas the reference vectors are taken from the Sun ephemeris, the known spacecraft orbit, the star catalogue, or the Earth's magnetic-field model, respectively. In practice, the measurement vectors (and, in fact, also the reference vectors) are tainted by measurement and modeling errors. If we ignore these errors, we can transform the reference vectors to the corresponding observed vectors by means of the (unknown) attitude matrix A, see Fig. 5:

$$\boldsymbol{v}_b^{(k)} = A\boldsymbol{v}_i^{(k)}, \quad k=1,2 \tag{8}$$

If the two measured vectors $\boldsymbol{v}_b^{(k)}$ are not parallel, they can be used to form an orthogonal coordinate frame with basis unit-vectors:

$$\boldsymbol{u}_1 = \boldsymbol{v}_b^{(1)}, \quad \boldsymbol{u}_2 = \boldsymbol{v}_b^{(1)} \times \boldsymbol{v}_b^{(2)} / |\boldsymbol{v}_b^{(1)} \times \boldsymbol{v}_b^{(2)}|, \quad \boldsymbol{u}_3 = \boldsymbol{u}_1 \times \boldsymbol{u}_2 \tag{9}$$

The 3×3 body matrix $M_{\text{body}} = [\boldsymbol{u}_1 \mid \boldsymbol{u}_2 \mid \boldsymbol{u}_3]$ repre-

sents the transformation between the $\boldsymbol{u}_j$ $(j=1, 2, 3)$ axes and the spacecraft body reference frame (Fig. 5).

In the same manner, the corresponding reference directions determine their own orthogonal frame:

$$\boldsymbol{U}_1=\boldsymbol{v}_i^{(1)},\quad \boldsymbol{U}_2=\boldsymbol{v}_i^{(1)}\times\boldsymbol{v}_i^{(2)}/|\boldsymbol{v}_i^{(1)}\times\boldsymbol{v}_i^{(2)}|,\quad \boldsymbol{U}_3=\boldsymbol{U}_1\times\boldsymbol{U}_2 \tag{10}$$

The 3×3 reference matrix $M_{\mathrm{ref}}=[\boldsymbol{U}_1\mid\boldsymbol{U}_2\mid\boldsymbol{U}_3]$ describes the transformation between the $\boldsymbol{U}_j$ $(j=1, 2, 3)$ vectors and the inertial reference frame. Equation (8) implies that $M_{\mathrm{body}}=A\,M_{\mathrm{ref}}$ and, because M_{ref} is orthogonal, $M_{\mathrm{ref}}^{-1}=M_{\mathrm{ref}}{}^{\mathrm{T}}$. The unknown attitude matrix A can thus be calculated immediately:

$$A=M_{\mathrm{body}}M_{\mathrm{ref}}{}^{\mathrm{T}} \tag{11}$$

This result is very attractive for on-board processing because of its inherent simplicity. Finally, it may be noted that the vector $\boldsymbol{v}_b^{(1)}$ is treated preferentially over $\boldsymbol{v}_b^{(2)}$ in the calculation of the body matrix. This is because the method implicitly ignores the information provided by the component of $\boldsymbol{v}_b^{(2)}$ along the direction of $\boldsymbol{v}_b^{(1)}$. Therefore, the vector $\boldsymbol{v}_b^{(1)}$ should preferably be the more accurate of the two measurement vectors.

4.2. QUEST Method

The deterministic TRIAD method presented above has two shortcomings. Only two measurement vectors can be treated at one time and part of the information delivered by the second vector is simply ignored. The QUEST (QUaternion ESTimator) method, on the other hand, computes the optimal attitude estimate from a set of n measurement vectors corrupted by measurement noise[3]. QUEST is the most frequently used batch method for three-axis attitude determination. It represents the solution of the Wahba problem[17] which is the origin of many modern algorithms for optimal three-axis attitude estimation[18].

The Wahba problem seeks the attitude matrix A that minimizes the loss-function $L(A)$, which represents the weighted-sum-square differences of the observed and the (rotated) reference vectors:

$$L(A)=\frac{1}{2}\sum_{k=1}^{n}w_k|\boldsymbol{v}_b^{(k)}-A\boldsymbol{v}_i^{(k)}|^2,\quad n\geq2 \tag{12}$$

The n weights w_k should be selected on the basis of the expected measurement errors in $\boldsymbol{v}_b^{(k)}$ $(k=1, \cdots, n)$ and they should be scaled according to $\Sigma_k(w_k)=1$. Equation (12) can be converted to the gain-function $g(A)=1-L(A)$ which must be maximized:

$$g(A)=\sum_{k=1}^{n}w_k(\boldsymbol{v}_b^{(k)\mathrm{T}}A\boldsymbol{v}_i^{(k)})=\mathrm{trace}\{AB^{\mathrm{T}}\} \tag{13a}$$

$$\text{with: } B=\sum_{k=1}^{n}w_k(\boldsymbol{v}_b^{(k)}\boldsymbol{v}_i^{(k)\mathrm{T}}) \tag{13b}$$

After expressing the attitude matrix A in terms of the quaternion $\boldsymbol{q}=(q_1, q_2, q_3, q_4)^{\mathrm{T}}$, and substituting this into equation (13a), we find a very attractive result for the gain function:

$$g(\boldsymbol{q})=\boldsymbol{q}^{\mathrm{T}}K\boldsymbol{q} \tag{14}$$

The 4×4 matrix K can be expressed in terms of the elements of the 3×3 matrix B of equation (13b):

$$K=\begin{pmatrix} B_{11}-B_{22}-B_{33} & B_{12}+B_{21} & B_{13}+B_{31} & B_{23}-B_{32} \\ B_{21}+B_{12} & B_{22}-B_{11}-B_{33} & B_{23}+B_{32} & B_{31}-B_{13} \\ B_{31}+B_{13} & B_{32}+B_{23} & B_{33}-B_{11}-B_{22} & B_{12}-B_{21} \\ B_{23}-B_{32} & B_{31}-B_{13} & B_{12}-B_{21} & B_{11}+B_{22}+B_{33} \end{pmatrix} \tag{15}$$

The problem of determining the optimal attitude has now been reduced to seeking the optimal quaternion $\boldsymbol{q}_{\mathrm{opt}}$ which maximizes the quadratic form in equation (14) under the constraint $|\boldsymbol{q}_{\mathrm{opt}}|=1$. It can be shown that $\boldsymbol{q}_{\mathrm{opt}}$ must be the eigenvector belonging to the largest eigenvalue $\lambda_{\max}$ of the matrix K. The QUEST method makes use of the fact that the maximum eigenvalue $\lambda_{\max}\approx1$ for any realistic batch of measurements. This condition can be understood after substituting the eigenvalue condition $K\boldsymbol{q}_{\mathrm{opt}}=\lambda_{\max}\boldsymbol{q}_{\mathrm{opt}}$ into equation (14). Because of the quaternion's normality property we find:

$$g(\boldsymbol{q}_{\mathrm{opt}})=(\boldsymbol{q}_{\mathrm{opt}})^{\mathrm{T}}\lambda_{\max}\boldsymbol{q}_{\mathrm{opt}}=\lambda_{\max} \tag{16}$$

The function $L(A_{\mathrm{opt}})$ in equation (12) represents the weighted-sum-square of the error contributions. When we use the optimal attitude matrix A_{opt} in the transformation from $\boldsymbol{v}_i^{(k)}$ into $\boldsymbol{v}_b^{(k)}$, we expect that $L(A)$ should normally be close to 0 and thus:

$$\lambda_{\max}=g(A_{\mathrm{opt}})=1-L(A_{\mathrm{opt}})\approx1 \tag{17}$$

This result may now be used as the starting value for calculating the exact eigenvalue $\lambda_{\max}$ through a numerical Newton-Raphson method. The quaternion $\boldsymbol{q}_{\mathrm{opt}}$ itself can be established with the help of the Gibbs vector and the Cayley-Hamilton theorem[3].

The QUEST method has been widely used in the attitude determination support of orbiting satellites. A number of alternatives to the QUEST method have been proposed in the literature[18] but the popularity of QUEST remains unbroken[19].

4.3. Kalman Filter Attitude Estimation

We mentioned in the Introduction that sequential optimal estimation methods[4-6] which are based on a Kalman Filter (KF) methodology, provide the most effective approaches for the determination of a time-varying attitude orientation. To ensure a proper KF performance an appropriate spacecraft dynamics model and an adequate observability of the attitude motion are essential. Reference 4) gives a good overview of the state of the art in KF estimation techniques for attitude determination in 1981 and it provides a useful general model with wide applicability.

Because of hardware limitations, the on-board processors of the 1980's could only handle linear KF estimation algorithms. Constant Kalman gain parameters were often used, which were established by extensive on-ground simulations. In this way, the HIPPARCOS satellite[20] achieved real-time on-board attitude knowledge of 1 arcsec (rms). The sensors used were mechanical rate-

integrating gyros plus a unique mission-specific star mapper in the telescope's focal plane. Furthermore, stringent autonomous thermal control of the entire optical payload was implemented.

With increasing hardware and software capabilities, the on-board use of nonlinear estimation methods like Extended Kalman Filters (EKF's) and Unscented Filters (UF's) have become feasible at present. Nowadays, hardly a satellite exists without one or more on-board estimators. Reference 5) provides a recent survey on nonlinear attitude estimation techniques. It contains 121 references and presents three different EKF's, namely the Multiplicative, Additive, and Backward-Smoothing Extended Kalman Filters. The first method remains the method of choice for most satellite applications. Unscented Filters offer attractive alternatives for applications with severe nonlinearities or when it is hard to calculate the partial derivatives.

5. LOW-COST ATTITUDE DETERMINATION AND CONTROL

During the last decade, the concept of using the geomagnetic field for determining and controlling a spacecraft's attitude has gained considerable popularity, in particular for small LEO satellites. This is because this concept has a low cost, uses low power, requires only low mass, and has no need for expendable propellants. Furthermore, the in-orbit operational reliability is also very favorable. There are many papers on this topic but References 21)-23) are of particular interest because they deal with actual satellite design and in-orbit operational experiences.

The satellite three-axis pointing orientation can be determined by a three-axis magnetometer measuring the three components of the Earth's magnetic field in the body frame, see Wertz[1], p. 361. Reference 24) presents a few attitude estimation algorithms which were developed for Kyushu University's QSAT satellite and may also be useful for other satellites in an Earth-pointing orientation.

Three-axis attitude control can be achieved by three mutually perpendicular magnetorquers (i.e., electromagnets). The torque is produced by electric currents running through a number of coils. The generated torque vector is described by $\boldsymbol{T}_a = \boldsymbol{M} \times \boldsymbol{B}$, which is the torque that actually can be produced (in contrast to the demanded control torque vector $\boldsymbol{T}_d$). The torque $\boldsymbol{T}_a$ acts normal to the magnetic field vector $\boldsymbol{B}$ and is also normal to the generated magnetic dipole moment vector $\boldsymbol{M}$ as shown in Fig. 6. The magnitude as well as the direction of the dipole moment $\boldsymbol{M}$ may be controlled by varying the currents in the coil loops or by adjusting the duty cycles of the three magnetorquers.

Unfortunately, the actual implementation of the control can be frustrating. Because the control torque can only act in a direction normal to the local geomagnetic field vector,

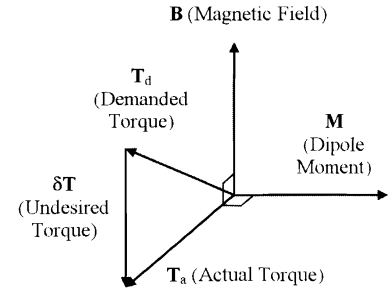

Fig. 6. Geometry of $\boldsymbol{B}$, $\boldsymbol{M}$, and torque vectors $\boldsymbol{T}_d$ and $\boldsymbol{T}_a$.

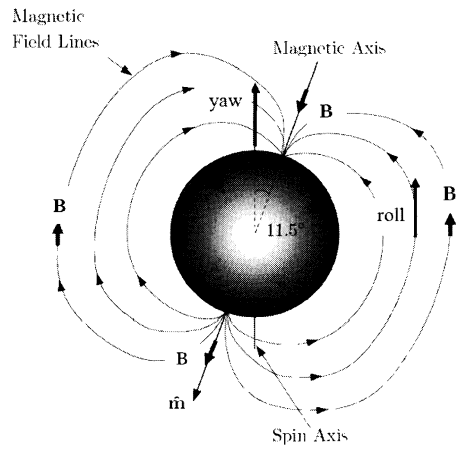

Fig. 7. Earth's magnetic field and attitude control deficiencies.

undesirable torque components are usually generated when trying to implement an arbitrary demanded torque vector (see Fig. 6).

A related issue is the fact that a specific required control torque can sometimes not be generated because the magnetic field vector happens to be pointing in an unfavorable direction. In particular, yaw errors cannot (or hardly) be controlled in the polar regions and roll errors in the equatorial regions (Fig. 7).

From a different point of view, a near-polar orbit is well suited for the geomagnetic control concept because the magnetic field vector varies periodically at twice the orbit rate. Therefore, the required torque vector for a specific demanded control actuation becomes available sometime during the orbit period (but possibly only after a considerable build-up of the attitude error).

For practical implementation, the demanded torque $\boldsymbol{T}_d$ may be calculated from the instantaneous attitude and rate errors with the help of a PD (Proportional-Derivative) control law[25]. As was noted above, however, this torque may not be oriented normal to the available $\boldsymbol{B}$ vector. An effective strategy would be to use the projection of $\boldsymbol{T}_d$ onto the plane normal to the $\boldsymbol{B}$ vector as the actual control torque $\boldsymbol{T}_a$ (see Fig. 6). In this way, the magnitude of the undesired torque component $\delta\boldsymbol{T}$ would be minimal. The final result for the required dipole $\boldsymbol{M}$ in terms of the demanded torque $\boldsymbol{T}_d$ follows from the geometry in Fig. 6:

$$\boldsymbol{M}=(\boldsymbol{B}\times\boldsymbol{T}_a)/B^2=(\boldsymbol{B}\times\boldsymbol{T}_d)/B^2 \quad (18)$$

Finally, we draw attention to the B-dot controller[26] which is a straightforward but very effective strategy for attitude acquisition (also known as detumbling) after the release of the satellite from the launcher. The principle of this controller is to minimize the rate of change $d\boldsymbol{B}/dt$ of the magnetic field vector as measured by the three-axis on-board magnetometers. Although the magnetic field vector itself varies over the orbit as shown in Fig. 7, the spacecraft tumbling rate following its orbit injection is typically much larger. Therefore, the rate of change in the measured $d\boldsymbol{B}/dt$ is essentially induced by the spacecraft body rate $\boldsymbol{\omega}_{sc}$.

The B-dot control law is designed to actuate opposite to the satellite attitude motion and is therefore able to reduce the rotational kinetic energy and to eventually stabilize the satellite:

$$\boldsymbol{M}=-C\,d\boldsymbol{B}/dt\approx -C(\boldsymbol{B}\times\boldsymbol{\omega}_{sc}) \quad (19)$$

A difficulty in the implementation of the B-dot controller is the fact that the vector $d\boldsymbol{B}/dt$ cannot be measured directly but must be derived from the magnetic measurements, for instance by using a discrete-time filter or a Kalman Filter estimator.

Finally, it should be kept in mind that the magnetometers and the magnetorquers should not be switched on simultaneously in order to prevent mutual interferences.

Acknowledgments

The author is grateful to Dr. Malcolm D. Shuster for helpful comments and criticisms.

REFERENCES

1) Wertz, J. R., ed.: Spacecraft Attitude Determination and Control, Springer Scientific + Business Media, Berlin and New York, 1978, Part III.
2) van der Ha, J. C.: Attitude Determination Covariance Analysis for Geostationary Transfer Orbits, J. Guid. Control Dynam., **9** (1986), pp. 156-163.
3) Shuster, M. D. and Oh, S. D.: Three-Axis Attitude Determination from Vector Observations, J. Guid. Control, **4** (1981), pp. 70-77.
4) Lefferts, E. J., Markley, F. L. and Shuster, M. D.: Kalman Filtering for Spacecraft Attitude Estimation, J. Guid. Control, **5** (1982), pp. 417-429.
5) Crassidis, J. L., Markley, F. L. and Chang, Y.: Survey of Nonlinear Attitude Estimation Methods, J. Guid. Control and Dynam., **30** (2007), pp. 12-28.
6) Shuster, M. D.: Kalman Filtering of Spacecraft Attitude and the QUEST Model, J. Astronaut. Sci., **38** (1990), pp. 377-393.
7) van der Ha, J., Rogers, G., Dellinger, W. and Stratton, J.: CONTOUR Phasing Orbits: Attitude Determination & Control Concepts and Flight Results, Adv. Astronaut. Sci., **114** (2003), Part II, pp. 767-781.
8) Shuster, M. D.: Efficient Algorithms for Spin-Axis Attitude Estimation, J. Astronaut. Sci., **31** (1983), pp. 237-249.
9) Tanygin, S. and Shuster, M. D.: Spin-Axis Attitude Estimation, J. Astronaut. Sci., **55** (2007), pp. 107-139.
10) van der Ha, J. C.: Equal-Chord Attitude Determination Method for Spinning Spacecraft, J. Guid. Control Dynam., **28** (2005), pp. 997-1005.
11) van der Ha, J. C.: The Two-Sun Cones Attitude Determination Method, J. Guid. Control Dynam., **31** (2008), pp. 1202-1209.
12) van der Ha, J. and Lappas, V.: Autonomous Attitude Determination and Control of Low-Cost Deep Space Probe, Proceedings of 6th IAA International Conference on Low-Cost Planetary Missions, Kyoto, Japan, 2005, pp. 169-176.
13) van der Ha, J. C.: Spin-Axis Attitude Determination Accuracy Model in the Presence of Biases, J. Guid. Control Dynam., **29** (2006), pp. 799-809.
14) van der Ha, J. C.: Models for Rhumb-Line Attitude Maneuvers and Error Propagation Effects, J. Guid. Control Dynam., **29** (2006), pp. 1384-1394.
15) Shuster, M. D.: A Survey of Attitude Representations, J. Astronaut. Sci., **41** (1993), pp. 439-517.
16) Black, H. D.: A Passive System for Determining the Attitude of a Satellite, AIAA J., **2** (1964), pp. 1350-1351.
17) Wahba, G.: Problem 65-1: A Least Squares Estimate of Spacecraft Attitude, SIAM Review, **7** (1965), p. 409.
18) Markley, F. L. and Mortari, D.: Quaternion Attitude Estimation using Vector Observations, J. Astronaut. Sci., **48** (2000), pp. 359-380.
19) Shuster, M. D.: The Quest for Better Attitudes, J. Astronaut. Sci., **54** (2006), pp. 657-683.
20) van der Ha, J. C.: Initial Attitude Determination for the HIPPARCOS Satellite, Acta Astronautica, **15** (1987), pp. 421-433.
21) Bak, T., Blanke, M. and Wisniewski, R.: Flight Results and Lessons Learned from the Oersted Attitude Control System, Proceedings of 4th ESA international Conference on Spacecraft Guidance, Navigation and Control Systems, ESTEC SP-425, 2000, pp. 87-94.
22) Steyn, W. H. and Hashida, Y.: In-Orbit Attitude and Orbit Control Commissioning of UoSAT-12, Proceedings of 4th ESA international Conference on Spacecraft Guidance, Navigation and Control Systems, ESTEC SP-425, 2000, pp. 95-101.
23) Steyn, W. H., Hashida, Y. and Lappas, V.: An Attitude Control System and Commissioning Results of the SNAP-1 Nanosatellite, Proceedings of 14th AIAA/USU Conference on Small Satellites, Utah State University, Logan, UT, USA, 2000, Paper SSC00-VIII-8.
24) Mimasu, Y., Narumi, T. and van der Ha, J. C.: Attitude Determination by Magnetometer and Gyros during Eclipse, AIAA/AAS Astrodynamics Specialist Conference, Honolulu, HI, USA, 2008, Paper AIAA-08-6932.
25) Miyata, K. and van der Ha, J. C.: Attitude Control using Magnetorquers, 19th AAS/AIAA Space Flight Mechanics Symposium, Savannah, GA, USA, 2009, Paper AAS-09-169.
26) Stickler, A. C. and Alfriend, K. T.: Elementary Magnetic Attitude Control System, J. Spacecraft Rockets, **13** (1976), pp. 282-287.

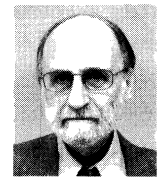

Jozef C. van der Ha (Member of JSASS)

Jozef van der Ha graduated from University of British Columbia, Vancouver, Canada, in 1977 with a Doctor degree in Mechanical Engineering. From 1977, he was Flight Dynamics specialist and, from 1986, Project Manager at ESA's Operations Center in Darmstadt, Germany. He contributed to the design and operations of ESA space missions (e.g.: METEOSAT's, ECS's, GIOTTO, HIPPARCOS, CASSINI-HUYGENS, and SOHO). From 1999, he was Consultant at Applied Physics Laboratory in USA for design and operations of CONTOUR mission. From 2004, he was Consultant at Surrey Satellite Technology Ltd. UK, for satellite system design. In April 2006, he joined Kyushu University as Professor. His major field of interest is satellite attitude determination and control. He is Senior Member of AIAA.